Article

Reduced Graphene Oxide Membrane induced Robust Structural Colors towards Personal Thermal Management

Zhijie Zhu, Jing Zhang, Yu-Long Tong, Gang Peng,
Tingting Cui, Cai-Feng Wang, Su Chen, and David A. Weitz

ACS Photonics, **Just Accepted Manuscript** • DOI: 10.1021/acsphotonics.8b00952 • Publication Date (Web): 15 Nov 2018

Reduced Graphene Oxide Membrane induced Robust Structural Colors towards Personal Thermal Management

Zhijie Zhu,[†‡] *Jing Zhang,*[†‡] *Yu-long Tong,*[†‡] *Gang Peng,*[†‡] *Tingting Cui,*[†‡] *Cai-Feng Wang,*[†‡] *Su Chen**[†‡] *and David A. Weitz**[§]

[†]State Key Laboratory of Materials-Oriented Chemical Engineering, College of Chemical Engineering and [‡]Jiangsu Key Laboratory of Fine Chemicals and Functional Polymer Materials, Nanjing Tech University, Nanjing 210009 (P. R. China)

[§]School of Engineering and Applied Science, Harvard University, 9 Oxford St, Cambridge, MA 02138, USA

KEYWORDS: graphene, structural color, angle-independent, human body cooling, thermal management

ABSTRACT: Angle-independent structural colors are prepared by membrane separation-assisted assembly (MSAA) method with modified reduced graphene oxide (rGO) as the substrate membrane. We show that the wrinkled and crumpled rGO laminates not only ensure uneven morphology of colloidal film but improve color

saturation by decreasing coherent scattering. In addition, we study the influence of stopband position on thermal insulation property of the colloidal film for the first time. High absolute temperature difference of 6.9 ^{o}C is achieved comparing with control sample. And films with longer stopband positions indicate better thermal insulation performance because of inherent slow photon effect in photonic structure. This general principle of thermal insulation by colloidal films opens the way to new generation of thermal management materials.

Structural colors, originating from interactions between periodical materials and light have received considerable attention due to their ability in controlling and manipulating light propagation.[1-2] Especially, amorphous colloidal particle arrays can also generate the photonic band gap,[3-5] which allow them to have constructive interference of scattered light and angle-independent behavior, thus presenting various applications in textile, paints, display and printing.[6-10] Up to now, much efforts have been done for the construction of angle-independent structural colors, such as spray-coating of colloidal latex,[11-13] fabrication of spherical colloidal crystal beads[14] and improving refractive index of microspheres.[15-16] Among them, making best of colloidal structures with short-range orders is of particular interest owing to its simplicity and scalability. In this respect, Song and Wang demonstrated an ultra-fast fabrication of large-scale colloidal photonic crystals via spray-coating method.[17] Ge et. al investigated the influence of constructive interference and Rayleigh scattering on formation of angle-independent

structural colors.[11, 18] More recently, Takeoka's group reported a layer-by-layer method for bio-inspired bright structurally colored colloidal amorphous arrays by controlling thickness and black background.[19] Despite significant achievements having been made in the preparation of amorphous structures, unmet challenges still remain. For instance, on one hand, the scalable methods that enabling structural colors forming in a fast and low-cost fashion. Another is how to take advantage of their stopbands, developing more new profound applications. In most cases, due to the evaporation-induced assembly that occurs at the liquid/air interface, the assembly progresses are time-consuming and insufficient for large-scale production. And the arising of transverse tensile stress from the capillary force could induce shrinkage of the colloidal film against a rigid substrate, along with cracks and poor structural colors.[20-21] Also, the brightness of most amorphous structures are severely decreased with the addition of light absorbers.[22-23] Thus, this motivates us to develop a new strategy for facilely producing amorphous structures with improved color saturation without sacrificing their brightness.

Recently, passive cooling technology with its ability in manipulating heat dissipations in a controllable fashion has been widely studied in indoor and outdoor thermal management.[24-26] In nature, the similar structures could be found in creatures such as elytra of longhorn beetles and the blue skin of the mandrill.[27-28] These structures result skin surface temperatures to be decreased via their thermal management performance, and then allow the creatures to be adapted to a hot environment. Although some researchers have made progress in developing body thermoregulators through the

matching of thermal emitter and the atmospheric transparency window or using well-designed nanoporous textiles to promote effective radiative cooling.[29-31] However, the utilizing of unique photonic structures to the best affection of outdoor thermal management is still in infancy and not yet fully explored.

Herein, inspired by this unique phenomenon, we developed a new kind of amorphous photonic structure representation of angle-independent structural colors by a membrane separation-assisted assembly (MSAA) strategy. Not only this method for construction of structural colors is uninvestigated, but also we applied the as-prepared structural color film to out-door thermal management applications for the first time, which is essential for personal cooling and energy saving. Reduced graphene oxide-sulfopropyl methacrylate potassium salt (rGO-SPM) substrate may greatly decrease the transverse tensile stress across the colloidal film. The resulting colloidal films are flexible and have uniform morphologies with improved structural colors. Nanoscale wrinkles and wave-like ripples on rGO-SPM caused by in-plane defects endow colloidal particles with amorphous arrangements. More importantly, the dark color rGO-SPM brought about during the reduction progress results in a decrease in coherent light scattering and reduction of light reflection from the substrate. That sharply improved color saturation of the colloidal film. By combining the synergetic effect of constructive scattering and slow photon, a maximal reduction of 6.9 ^{o}C was achieved when exposing to sun radiation. This finding opens a new pathway for fabrication of amorphous colloidal structures with the construction of personal thermal management by structural colors.

RESULTS AND DISCUSSION

Different from evaporation induced self-assembly of traditional structural colors, our strategy adopts MSAA method to fabricate uniform structural colors. We present here an easy-to-perform and versatile method enabling colloidal film forming onto a robust membrane. That is, we initially synthesized sulfonated rGO by using sulfopropyl methacrylate potassium salt (SPM) grafting onto rGO via in situ free radical polymerization (Figure 1a, Figure S1 and S2). Then, in a typical run, rGO-SPM nanosheets were assembled into separation layer on a porous mixed cellulose ester (MCE) filter (Figure S11). Straight after, the colloidal film formation is done by vacuum filtering of dilute monodisperse colloidal poly(styrene- methyl methacrylate-acrylic acid) (poly(St-MMA-AA)) suspension (0.1-5 wt%, 3-5 mL) through an rGO-SPM membrane, followed by air drying and peeling off from the filter (Figure S12). This progress takes less than 2 minutes, comparing with traditional evaporation-induced colloidal film-forming processes (typically several hours for vertical deposition).[33, 34] Figure 1b and 1c present the schematic comparison of MSAA process and conventional evaporation-induced colloidal film-forming progress. The construction of conventional structural colors is highly dependent on colloid evaporating on rigid substrates and the assembly process mostly takes place at the liquid/air interfaces. When the environment temperature and concentration of colloids are low, it will affect film forming time, and even result in uneven crack assembly. Thus, this traditional method is time consuming and not easily scaled up because

dehydration of colloids is more difficult (Figure 1b).[35-36] Alternatively, by MSAA method, we facilely remove water from colloidal latex by using rGO-SPM as the substrate membrane under vacuum condition (Figure 1c). This MSAA method can greatly decrease film-forming time and the occurrence of cracks. Also, the soft and wrinkle-like rGO-SPM structure may greatly break the outward capillary flow, allowing consecutive and symmetrical colloidal film forming.

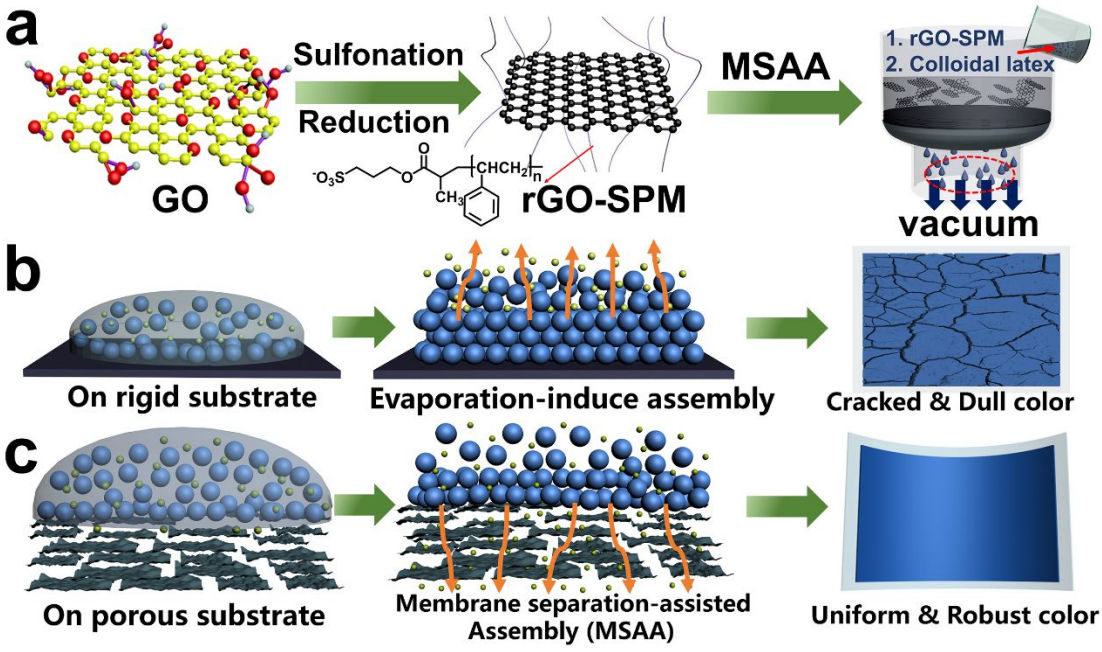

Figure 1. (a) Schematic illustration of the fabrication of rGO-SPM and assembly progress of the rGO-SPM/poly(St-MMA-AA) membranes via membrane separation-assisted assembly (MSAA) method. Herein, the method comprises two steps. The first step is the assembly of rGO on a filter paper. The second step is membrane filtration of colloidal latex. (b) Schematic illustration of evaporation-induce assembly. Cracks along with dull structural color could always be observed. (c) Schematic illustration of MSAA method. The method is facile of achieving uniform structural colors.

The transmission electron microscope (TEM) image of rGO-SPM is shown in Figure S3, and the sheet-like nature of product is well reserved. Analytical results from UV-Vis absorption, thermogravimetric analysis (TGA), derivative thermogravimetry (DTG), x-ray diffraction (XRD) spectra, Raman spectra, FT-IR spectra, and X-ray photoemission spectroscope (XPS) reveal that SPM was successfully grafted onto the surface of rGO, and the de-oxygenation of GO was successfully done (Detailed discussions of these results can be found in the supporting information, Figure S4-S10). The optical and SEM images of rGO-SPM membrane are shown in Figure 2a-c. The pristine rGO-SPM membrane exhibits a compacted laminar and layer by layer architecture on its cross-section (Figure 2b). Meanwhile, surface SEM of rGO-SPM membrane displays nanoscale wrinkles and wave-like ripples (Figure 2c). More importantly, the as-prepared rGO-SPM membrane exhibits better wettability (water contact angle of 79.5^{o}), comparing with 100.2^{o} of control rGO sample (Figure S13). This may be mechanistically related to the better performance of structural color fabrication, which will be discussed below. After filtration and assembly of poly(St-MMA-AA) microspheres, the as-prepared colloidal film exhibits uniform structural color (Figure 2d and S14) and could be bent at any directions showing preeminent flexibility (Figure S15). As seen in Figure S16, colloidal latices with different concentrations (0.2 wt%, 0.5 wt%, 1 wt%, 2 wt% and 5 wt%) were deposited on rGO-SPM membranes, respectively. It is obvious that the hue is highly dependent on the thickness (calculated by formula 2) of the particle arrays (Figure S17). Typical surface and cross-sectional image of rGO-SPM/poly(St-MMA-AA) membrane is shown in

Figure 2e, f. The rGO-SPM/poly(St-MMA-AA) show a hierarchical structure and the microspheres are closely packed with a thickness of ~1.0 μm. The particles are isotropically distributed with short-range order (Figure 2e and Figure S24). Also, the ring-shaped pattern in 2D fast Fourier transform (2D FFT) image (inset of Figure 3e) reveals that the particles form an amorphous array, consisting with the SEM images.[37]

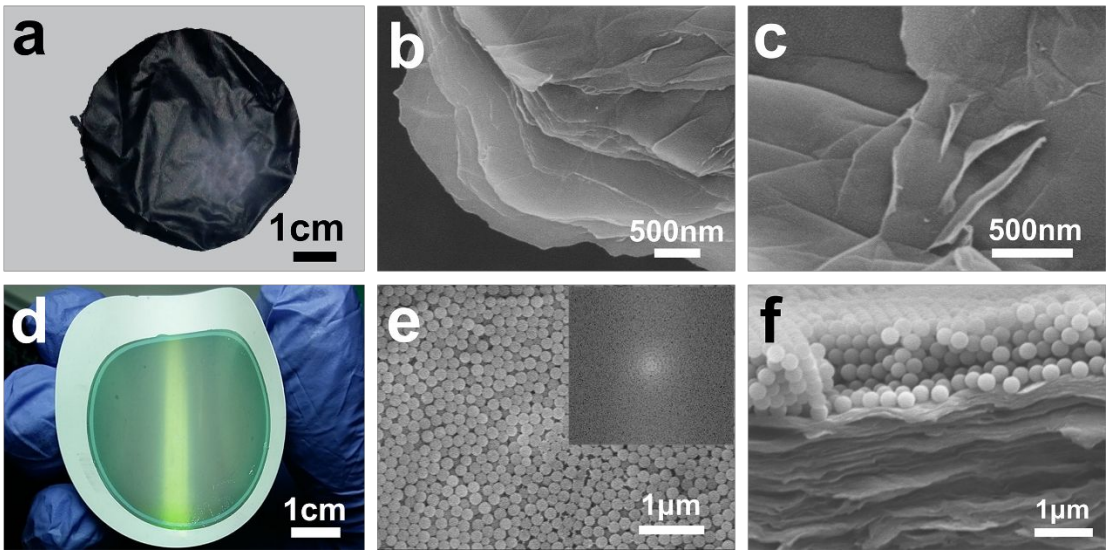

Figure 2. (a) Photograph of an rGO-SPM membrane. SEM images of cross-section (b) and surface (c) of an rGO-SPM/poly(St-MMA-AA) membrane. (d) Photograph of a structural color film prepared by MSAA. Corresponding SEM images of the surface (e) and cross-section (f). Insert: the corresponding FFT image.

Figure 3a presents optical images of three different colloidal films, which are composed of poly(St-MMA-AA) microspheres with diameters of 195 nm, 218 nm and 256 nm (Figure S18), respectively. These colloidal films display virtually identical structural colors at the view angles changing from 90° to 30°, whilst the colloidal film prepared by vertical deposition sharply varies from red to green (Figure S19, S20). To visually

characterize the angle dependence of the colloidal films, the angle-resolved reflection spectra and their corresponding contour maps were measured.[38] As shown in Figure 3b, band positions of colloidal films prepared by MSAA barely shift (less than 5 nm) when the incident angle varies from 90° to 30°, indicating angle-independent property. Meanwhile, the corresponding contour maps with reflection wavelength (λ) on the x axis, view angle (θ) on the y axis and reflection intensity (I) being converted to colors in maps also prove their angle-independent behavior. The contour maps of colloidal films prepared by MSAA exhibit consecutive and linear reflection bands that are vertical to x axises. As compared in Figure S21, the contour map of colloidal film obtained from vertical deposition splits into different regions due to the reflection band shift demonstrating the highly-ordered nature of ordinary periodic colloidal structures.

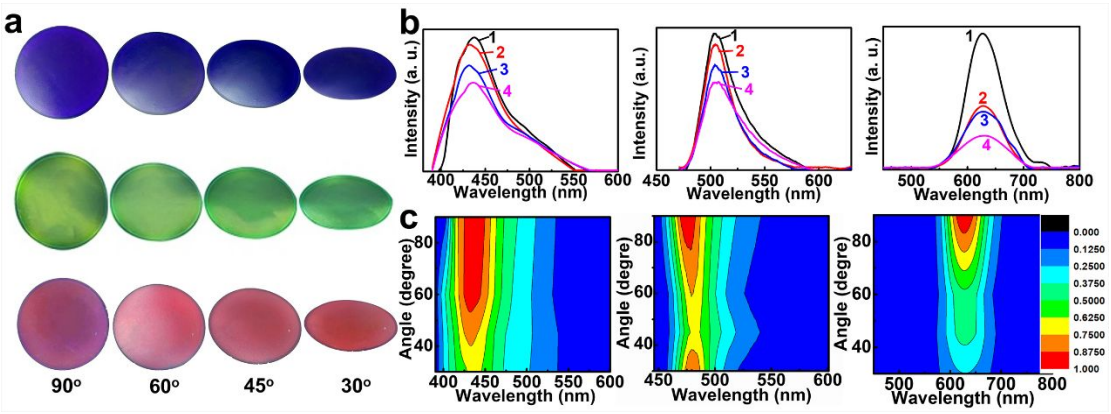

Figure 3. (a) Photographs of three different colloidal films observed at angles from 90° to approximately 30°. (b) Reflection spectra of colloidal films obtained at incident angles of 90° (curve 1), 60° (curve 2), 45° (curve 3), 30° (curve 4) and (c) corresponding contour maps.

Interestingly, the as-prepared colloidal films show enhanced color saturation compared with control sample (Figure 4 and Figure S22). To better understand the origin of this enhanced structural color, colloidal microspheres were deposited on blank filter paper for comparison (by filtrating of diluted colloidal latex (0.1-5 wt%, 3-5 mL) on a MCE filter paper under vacuum condition). As a matter of fact, the angle-independent photonic pseudogap is mainly caused by constructive interference of scattered light from the amorphous array, while the ordinary photonic pseudogap is mainly caused by Bragg diffraction from ordered lattice arrangement.[3, 39-40] The transmitted light (40-60 %, Figure S23) from the other side of the filter paper greatly disrupts Bragg reflection caused by the microsphere array, resulting in pale structural color. However, the black rGO-SPM that is brought about during the reduction process prohibits the transmitted light and ensures the interference of coherent scattering light from amorphous arrays (Figure 4a, b). Thus, the color saturation of this colored film could be remarkably reinforced.

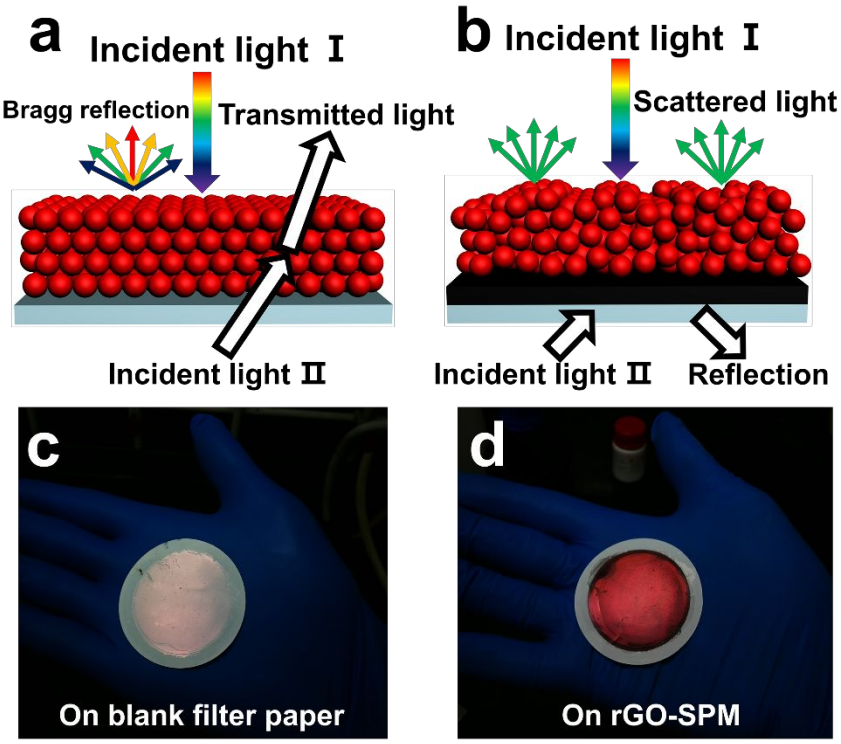

Figure 4. Schematic illustration of the formation of the structural color on blank filter paper (a) and rGO-SPM (b). Photographs of poly(St-MMA-AA) microspheres deposit on blank filter paper (c) and rGO-SPM (d).

The second set of experiments was focused on studying the passive cooling of structural color film. Benefiting from the angle-independent structural colors and inherent stopband behavior, these colloidal films show potential for outdoor personal thermal insulation. In fact, the recent studies of many natural examples have revealed that highly ordered architectures could efficiently dissipate heat back to the surroundings and keep the body cool.[41-42] For example, Cataglyphis bombycina, the silver ants that survive in Sahara desert can reduce heat absorption by reflecting large portion of solar radiation on a dense array of triangular hairs.[25] Inspired by these features, we studied the impact of stopband position on the efficiency of thermal insulation. To evaluate the influence

of stopband positions on heat dissipation process, 8 individual structural colors that are composed of poly(St-MMA-AA) microspheres with different corresponding diameters are prepared (Figure S25). The obtained colors, covering the whole visible light regime are derived from MSAA method and are uniform and independent of viewing angles as demonstrated above. In a typical procedure, a colloidal film with a diameter of 50 mm was placed on top the shelf (obtained from a 3D printer). Under natural sun light radiation, the temperature of structural color film with stopband centered at 650 nm, increased from 24.6 ^{o}C to 34.3 ^{o}C within 360 s. In contrast, the bulk polystyrene film without a structural color showed a rapid temperature increase from 24.6 ^{o}C to 45.5^{o}C. The infrared photographs of sample films after 15 min of irradiation are shown in Figure 5a. The inserts are temperature differences (ΔT) between different sample surfaces (T_{sample}) and the cement floor background (T_{floor}). With the increase of stopband position, ΔT appears a downward trend (Figure S26 and S27). The stopband of a structural color film that inhibit certain wavelength propagation is the main reason for this result. The structural color films that possess red or near-infrared colors can prohibit more longer-wavelength light from absorption. For a more realistic case, we adopted structural color film to integrate on human skin, where the film was attached to a human hand. Figure 5d-f are human hands with structural color film (stopband centered at 650 nm), rGO-SPM film and bulk polystyrene film (without a color), respectively. Before measurement, all samples are in thermal equilibrium after solar radiation for at least 15 min. The temperature of bulk polystyrene film and rGO-SPM was 33.5 ^{o}C and 38.1 ^{o}C, respectively. On contrary, for structural color film, the

temperature was maintained at 32.3 °C, lower than skin temperature 37.8 °C. This is consistent with the above results. It is worthwhile to note that our structural color film is composed of two sides: the structural color side and the black rGO-SPM side. It is expected that the color side can be processed to decrease solar radiation in summer, while the black rGO-SPM side been processed to absorb more in winter. These findings, together with the demand of suppressing solar irradiance during the daytime, offers new insight into functional and scalable textile for personal cooling and energy saving.

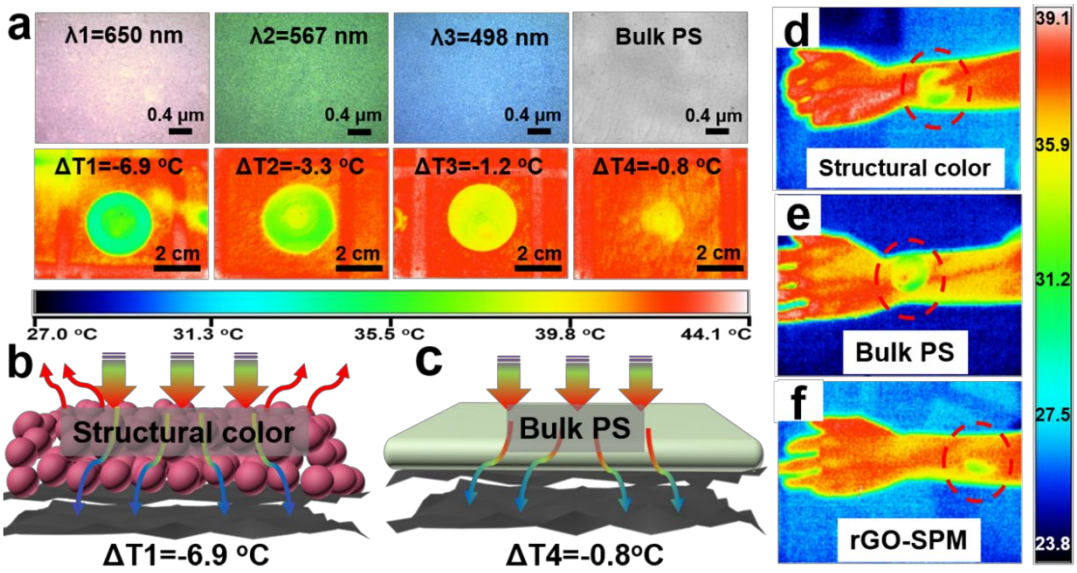

Figure 5. (a) Structural colors prepared by MSAA by varying the diameters of poly(St-MMA-AA) and corresponding infrared photographs after 15 min of irradiation. Schematics of comparison between (b) structural color film and (c) bulk polystyrene film. Infrared images of (d) structural color film, (e) bulk polystyrene film and (f) rGO-SPM (attached to human body) under radiation.

Structural color patterns that are free from photobleaching represent an important application of photonic crystals.[43-44] This MSAA method was also utilized to construct

angle-independent structural color patterns. As shown in Figure S28, a tubular photonic structure on inner surface of a commercial ceramic tube with average pore size of 0.2 μm is presented by placing it in vacuum circumstance. It exhibits uniform structural color along diametrical direction. This tubular colloidal structure derived from MSAA method may find potential use in obtaining monochromatic transmitted light, as long as the photonic band gap (PBG) meets the critical value.[45] Furthermore, by combining this method with microfluidic printing, a well-defined structural color matrix could be easily realized (Figure S29). Multi-color photonic patterns can be easily achieved with assistance of mask lithography technology. In our experiment, a specially designed mask (obtained by a 3D printer, Figure S30) was placed under as prepared rGO-SPM membrane. Colloidal latex was then filled with lower regions and vacuum filtered until water totally permeated. Afterwards, additional pattern was fabricated in the same manner with another mask (Figure S31). Such structural colors that are composed of 1D to 3D colloidal structures are of great significance in self-assembly of colloidal particles for practical application involving displays and monochromatic optical filters.

CONCLUSIONS

In summary, we report a membrane separation-assisted assembly (MSAA) strategy for the construction of angle-independent structural colors. By taking advantage of the water transport channels in sulfonated rGO, water and submicron particles could be separated easily, along with colloidal particles assembles into amorphous structures. Moreover, the color contrast is greatly enhanced by the rGO-SPM background.

Accordingly, the resulting colloidal films are crack-free and could be bent at any directions showing preeminent flexibility. Comparing with conventional evaporation-induced techniques, MSAA method provides an easy-to-perform solution to assembly of colloidal particles. We also investigated the influence of structural colors on thermal insulation and applied it to personal thermal management for the first time. A maximal reduction of 6.9 ^{o}C can be achieved when the stopband of structural color is centered at 650 nm. Such colloidal films with angle-independent structural colors may provide applications in photoelectric material and new generation of out-door thermal management materials. More parallel experiments for personal cooling and energy saving by using structural colors will continue.

Materials and Methods

Materials. Methyl methacrylate acrylic acid (MMA, 98%), acrylic acid (AA, 98%), $KMnO_4$, H_3PO_4 and H_2O_2 (AR, 30 wt% in water) were purchased from Sinopharm Chemical Reagent Co., Ltd. (Shanghai, China). Styrene (St, 99%), potassium persulfate (KPS, 99%), polyvinylpyrrolidone (PVP, K40, M_w= 40000), Sulfopropyl methacrylate potassium salt (SPM, 95%), Graphite (120 mesh) were received from Aladdin Industrial Corporation. Purified water with a resistance greater than 18 MΩ*cm was used throughout the experiments. Styrene was purified by distillation under a reduced vacuum to remove inhibitor before usage. All other chemicals were used as received.

Synthesis of poly(styrene- methyl methacrylate- acrylic acid) (Poly(St-MMA-AA)) colloidal particles. The monodispered poly(St-MMA-AA) microspheres were synthesized via our previous method and are used in whole study. Briefly, 0.24 g of PVP, 0.3 g of NaHCO3, were dissolved in 110 g of deionized water in a 250 mL round flask with stirring under nitrogen atmosphere. 6.0 g of St and 0.04 g of KPS dissolved in 12 g deionized water was add into the solution dropwise after the mixture was heated at 98 ^{o}C. The reaction was continued for another 1.5 h; and then, 0.5 g of MMA, 0.5g of AA and 0.01 g of KPS dissolved in 10g water were added, and the reaction was continued for another 5 h.

Synthesis of rGO-SPM composite. The rGO-SPM composite was synthesized via in situ free radical polymerization. The reduction of GO and graft of SPM was carried out simultaneously: 0.2 g of SPM was added into graphene oxide aqueous solution (50 mg of graphene oxide dissolved in 50 g water) and sonicated (40 kHz) for 1 h to obtain a homogeneous solution. After the solution was purged with N_2 for 30 min and heated to 85 ^{o}C, 0.035 g of KPS dissolved in 10 g deionized water was add into the solution dropwise to initiate the polymerization. Meanwhile, 44 μL of hydrazine hydrate and 700 μL of ammonium hydroxide were added into the solution to reduce the graphene oxide. The reaction was continued overnight.

Membrane separation-assisted assembly process for angle-independent structural color films. The angle-independent structural color films were prepared by filtering rGO-SPM solution and colloidal suspension alternatively. Firstly, 2-4 mL of as

synthesized rGO-SPM aqueous solution was filter through a mixed cellulose ester filter membrane (47 mm in diameter, 0.2 μm pore size). Then, 4-6 ml the diluted colloidal suspension with a concentration of 0.2 wt% was dropped on the rGO- SPM film carefully and filtered until dry.

Preparation of structural color patterns. A stepwise filtration method was adopted here to prepare structural color patterns. The first layer of structural color pattern was prepared by mask Ⅰ (this mask was obtained by a 3D-printer). After the first layer of structural color pattern was dry and mask Ⅰ was replaced by mask Ⅱ, the second layer of structural color pattern was prepared by the same way.

Preparation of structural color matrix by microfluidic printing method. Typically，the emulsion of 15 wt% poly(St-MMA-AA) were injected into a needle (inner diameter: 5μm). The flow rates were kept at 0.6 mL h^{-1}. Subsequently, droplets were printed on the as prepared rGO-SPM paper by a 3D printing machine. Finally, poly(St-MMA-AA) microspheres were self-assembled into PC structure after the solvent evaporation.

Characterization. The XRD patterns were recorded on a BrukerD8 Advance X-ray diffractometer (40 kV, 25 mA, Cu Kα radiation, λ=1.5418 Å) at room temperature. Fourier transform infrared (FT-IR) spectra were recorded on a Nicolet 6700 FT-IR spectrometer. IR images were performed on a Thermo Scientific Nicolet iN10 infrared microscope equipped with a liquid nitrogen cooled MCT detector (Thermo Electron Corporation, USA). Ultraviolet-visible (UV-vis) spectrum was obtained using a Perkin-

Elmer Lambda 900 UV-vis spectrometer. The morphologies of materials were observed by scanning electron microscopy (SEM) using a HITACHI S-4800 scanning electron microscope. Low-resolution Transmission Electron Microscopy (TEM) images were recorded on a JEOL JEM 1011 microscope operating at 100 kV. Atomic force microscopy (AFM) images was accomplished under ambient conditions with Bruker Dimension Icon scanning probe microscope in the tapping mode of operation. Reflection spectra were recorded using an optical microscope equipped with a fiber optic spectrometer (Ocean Optics, USB4000). Contact angles were measured with a KRÜSS DSA100 (KRÜSS, Germany) contact-angle system at ambient temperature. The samples for thermogravimetric analysis (TGA) were prepared by drying under vacuum for water removal, and the analysis was carried out at a heating rate of 5 ^{o}C min^{-1} from 30 to 700 ^{o}C in the N_2 atmosphere. X-ray photoelectron spectroscopy (XPS) measurements were carried out on an ES-CAIAB250 XPS system with Al/Kα as the source, and the energy step size was set as 0.100 eV. The size and zeta potential of materials were measured by dynamic light scattering (DLS) (Malvern, ZEN3690). Temperature profiles were measured using a Fluke Ti30 IR thermal imager.

ASSOCIATED CONTENT

The Supporting information is available free of charge on the ACS Publications website at http://pubs.acs.org/

AUTHOR INFORMATION

Corresponding Author

*E-mail: chensu@njtech.edu.cn

*E-mail: weitz@seas.harvard.edu

Notes

The authors declare no competing financial interest.

ACKNOWLEDGMENT

This work was supported by National Natural Science Foundation of China (21736006, 21474052), National Key Research and Development Program of China (2016YFB0401700), Natural Science Foundation of Jiangsu Province (BK20171013) and Priority Academic Program Development of Jiangsu Higher Education Institutions (PAPD). Fund of State Key Laboratory of Material-Oriented Chemical Engineering (ZK201704).

REFERENCES

1. van Blaaderen, A., Materials science - Opals in a new light. *Science* **1998,** *282*, 887-888.

2. von Freymann, G.; Kitaev, V.; Lotschz, B. V.; Ozin, G. A., Bottom-up assembly of photonic crystals. *Chem. Soc. Rev.* **2013,** *42*, 2528-2554.

3. Noh, H.; Liew, S. F.; Saranathan, V.; Mochrie, S. G. J.; Prum, R. O.; Dufresne, E. R.; Cao, H., How Noniridescent Colors Are Generated by Quasi-ordered Structures of Bird Feathers. *Adv. Mater.* **2010,** *22*, 2871-2880.

4. Takeoka, Y., Angle-independent structural coloured amorphous arrays. *J. Mater. Chem.* **2012,** *22*, 23299-23309.

5. Shi, L.; Zhang, Y.; Dong, B.; Zhan, T.; Liu, X.; Zi, J., Amorphous Photonic Crystals with Only Short-Range Order. *Adv. Mater.* **2013,** *25*, 5314-5320.

6. Chen, F.; Yang, H.; Li, K.; Deng, B.; Li, Q.; Liu, X.; Dong, B.; Xiao, X.; Wang, D.; Qin, Y.; Wang, S.-M.; Zhang, K.-Q.; Xu, W., Facile and Effective Coloration of Dye-Inert Carbon Fiber Fabrics with Tunable Colors and Excellent Laundering Durability. *Acs Nano* **2017,** *11*, 10330-10336.

7. Hang, Z.; Mu, Z.; Li, B.; Wang, Z.; Zhang, J.; Niu, S.; Ren, L., Active Antifogging Property of Monolayer SiO2 Film with Bioinspired Multiscale Hierarchical Pagoda Structures. *Acs Nano* **2016,** *10*, 8591-8602.

8. Li, Q.; Zhang, Y.; Shi, L.; Qiu, H.; Zhang, S.; Qi, N.; Hu, J.; Yuan, W.; Zhang, X.; Zhang, K.-Q., Additive Mixing and Conformal Coating of Noniridescent Structural Colors with Robust Mechanical Properties Fabricated by Atomization Deposition. *Acs Nano* **2018,** *12*, 3095-3102.

9. Arsenault, A. C.; Puzzo, D. P.; Manners, I.; Ozin, G. A., Photonic-crystal full-colour displays. *Nat. Photon.* **2007,** *1*, 468-472.

10. Bao, B.; Li, M.; Li, Y.; Jiang, J.; Gu, Z.; Zhang, X.; Jiang, L.; Song, Y., Patterning fluorescent quantum dot nanocomposites by reactive inkjet printing. *Small* **2015,** *11*, 1649-54.

11. Yang, X.; Ge, D.; Wu, G.; Liao, Z.; Yang, S., Production of Structural Colors with High Contrast and Wide Viewing Angles from Assemblies of Polypyrrole Black Coated Polystyrene Nanoparticles. *ACS Appl. Mater. Interfaces* **2016,** *8*, 16289-16295.

12. Ge, D.; Lee, E.; Yang, L.; Cho, Y.; Li, M.; Gianola, D. S.; Yang, S., A Robust Smart Window: Reversibly Switching from High Transparency to Angle-Independent Structural Color Display. *Adv. Mater.* **2015,** *27*, 2489-2495.

13. Ge, D.; Yang, L.; Wu, G.; Yang, S., Spray coating of superhydrophobic and angle-independent coloured films. *Chem. Commun.* **2014,** *50*, 2469-2472.

14. Gu, H.; Zhao, Y.; Cheng, Y.; Xie, Z.; Rong, F.; Li, J.; Wang, B.; Fu, D.; Gu, Z., Tailoring Colloidal Photonic Crystals with Wide Viewing Angles. *Small* **2013,** *9*, 2266-2271.

15. Han, M. G.; Shin, C. G.; Jeon, S. J.; Shim, H.; Heo, C. J.; Jin, H.; Kim, J. W.; Lee, S., Full Color Tunable Photonic Crystal from Crystalline Colloidal Arrays with an Engineered Photonic Stop‐Band. *Adv. Mater.* **2012,** *24*, 6438-6444.

16. Su, X.; Xia, H.; Zhang, S.; Tang, B.; Wu, S., Vivid structural colors with low angle dependence from long-range ordered photonic crystal films. *Nanoscale* **2017,** *9*, 3002-3009.

17. Cui, L.; Zhang, Y.; Wang, J.; Ren, Y.; Song, Y.; Jiang, L., Ultra-Fast Fabrication of Colloidal Photonic Crystals by Spray Coating. *Macromol. Rapid Commun.* **2009,** *30*, 598-603.

18. Ge, D.; Yang, L.; Wu, G.; Yang, S., Angle-independent colours from spray coated quasi-amorphous arrays of nanoparticles: combination of constructive interference and Rayleigh scattering. *J. Mater. Chem. C* **2014,** *2*, 4395-4400.

19. Iwata, M.; Teshima, M.; Seki, T.; Yoshioka, S.; Takeoka, Y., Bio-Inspired Bright Structurally Colored Colloidal Amorphous Array Enhanced by Controlling Thickness and Black Background. *Adv. Mater.* **2017,** *29*, 1605050-n/a.

20. Huang, Y.; Zhou, J.; Su, B.; Shi, L.; Wang, J.; Chen, S.; Wang, L.; Zi, J.; Song, Y.; Jiang, L., Colloidal Photonic Crystals with Narrow Stopbands Assembled from Low-Adhesive Superhydrophobic Substrates. *J. Am. Chem. Soc.* **2012,** *134*, 17053-17058.

21. Zhu, Z.; Zhang, J.; Wang, C.-F.; Chen, S., Construction of Hydrogen-Bond-Assisted Crack-Free Photonic Crystal Films and Their Performance on Fluorescence Enhancement Effect. *Macromol. Mater. Eng.* **2017,** *302*, 1700013.

22. Zhang, Y.; Dong, B.; Chen, A.; Liu, X.; Shi, L.; Zi, J., Using Cuttlefish Ink as an Additive to Produce Non-iridescent Structural Colors of High Color Visibility. *Adv. Mater.* **2015,** *27*, 4719-4724.

23. Takeoka, Y.; Yoshioka, S.; Takano, A.; Arai, S.; Nueangnoraj, K.; Nishihara, H.; Teshima, M.; Ohtsuka, Y.; Seki, T., Production of Colored Pigments with Amorphous Arrays of Black and White Colloidal Particles. *Angew. Chem. Int. Ed.* **2013,** *52*, 7261-7265.

24. Gao, T.; Yang, Z.; Chen, C.; Li, Y.; Fu, K.; Dai, J.; Hitz, E. M.; Xie, H.; Liu, B.; Song, J.; Yang, B.; Hu, L., Three-Dimensional Printed Thermal Regulation Textiles. *ACS nano* **2017**.

25. Hsu, P.-C.; Liu, X.; Liu, C.; Xie, X.; Lee, H. R.; Welch, A. J.; Zhao, T.; Cui, Y., Personal Thermal Management by Metallic Nanowire-Coated Textile. *Nano Lett.* **2015,** *15*, 365-371.

26. Hsu, P.-C.; Song, A. Y.; Catrysse, P. B.; Liu, C.; Peng, Y.; Xie, J.; Fan, S.; Cui, Y., Radiative human body cooling by nanoporous polyethylene textile. *Science* **2016,** *353*, 1019-1023.

27. Prum, R. O.; Torres, R. H.; Williamson, S.; Dyck, J., Coherent light scattering by blue feather barbs. *Nature* **1998,** *396*, 28.

28. Shi, N. N.; Tsai, C.-C.; Camino, F.; Bernard, G. D.; Yu, N.; Wehner, R., Keeping cool: Enhanced optical reflection and radiative heat dissipation in Saharan silver ants. *Science* **2015,** *349*, 298-301.

29. Cui, Y.; Gong, H.; Wang, Y.; Li, D.; Bai, H., A Thermally Insulating Textile Inspired by Polar Bear Hair. *Adv. Mater.* **2018,** *30*.

30. Yang, A.; Cai, L.; Zhang, R.; Wang, J.; Hsu, P.-C.; Wang, H.; Zhou, G.; Xu, J.; Cui, Y., Thermal Management in Nanofiber-Based Face Mask. *Nano Lett.* **2017,** *17*, 3506-3510.

31. Chen, Z.; Zhu, L.; Raman, A.; Fan, S., Radiative cooling to deep sub-freezing temperatures through a 24-h day-night cycle. *Nat. Commun.* **2016,** *7*.

32. Feng, H.; Cheng, R.; Zhao, X.; Duan, X.; Li, J., A low-temperature method to produce highly reduced graphene oxide. *Nat. Commun.* **2013,** *4*, 1539.

33. Zhong, Q.; Xie, Z.; Ding, H.; Zhu, C.; Yang, Z.; Gu, Z., Carbon Inverse Opal Rods for Nonenzymatic Cholesterol Detection. Small 2015, 11 (43), 5766-5770.

34. Russell, J. L.; Noel, G. H.; Warren, J. M.; Tran, N.-L. L.; Mallouk, T. E., Binary Colloidal Crystal Films Grown by Vertical Evaporation of Silica Nanoparticle Suspensions. Langmuir 2017, 33 (39), 10366-10373.

35. Dai, Z.; Li, Y.; Duan, G.; Jia, L.; Cai, W., Phase Diagram, Design of Monolayer Binary Colloidal Crystals, and Their Fabrication Based on Ethanol-Assisted Self-Assembly at the Air/Water Interface. *ACS Nano* **2012,** *6*, 6706-6716.

36. Gallego-Gómez, F.; Blanco, A.; López, C., Exploration and Exploitation of Water in Colloidal Crystals. *Adv. Mater.* **2015,** *27*, 2686-2714.

37. Yi, B.; Shen, H., Facile fabrication of crack-free photonic crystals with enhanced color contrast and low angle dependence. *J. Mater. Chem. C* **2017,** *5*, 8194-8200.

38. Zhang, Y.; Fu, Q.; Ge, J., Photonic sensing of organic solvents through geometric study of dynamic reflection spectrum. *Nat. Commun.* **2015,** *6*, 7510.

39. Lee, I.; Kim, D.; Kal, J.; Baek, H.; Kwak, D.; Go, D.; Kim, E.; Kang, C.; Chung, J.; Jang, Y.; Ji, S.; Joo, J.; Kang, Y., Quasi-Amorphous Colloidal Structures for Electrically Tunable Full-Color Photonic Pixels with Angle-Independency. *Adv. Mater.* **2010,** *22*, 4973.

40. von Freymann, G.; Kitaev, V.; Lotsch, B. V.; Ozin, G. A., Bottom-up assembly of photonic crystals. *Chem. Soc. Rev.* **2013,** *42*, 2528-2554.

41. Bai, H.; Chen, Y.; Delattre, B.; Tomsia, A. P.; Ritchie, R. O., Bioinspired large-scale aligned porous materials assembled with dual temperature gradients. *Sci. Adv.* **2015,** *1*, 8.

42. Catrysse, P. B.; Song, A. Y.; Fan, S., Photonic Structure Textile Design for Localized Thermal Cooling Based on a Fiber Blending Scheme. *ACS Photonics* **2016,** *3*, 2420-2426.

43. Chen, K.; Fu, Q.; Ye, S.; Ge, J., Multicolor Printing Using Electric-Field-Responsive and Photocurable Photonic Crystals. *Adv. Funct. Mater.* **2017**, 1702825.

44. Chen, M.; Tian, Y.; Zhang, J.; Hong, R.; Chen, L.; Chen, S.; Son, D. Y., Fabrication of crack-free photonic crystal films via coordination of microsphere terminated dendrimers and their performance in invisible patterned photonic displays. *J. Mater. Chem. C* **2016,** *4*, 8765-8771.

45. Fu, Q.; Chen, A.; Shi, L.; Ge, J., A polycrystalline SiO 2 colloidal crystal film with ultra-narrow reflections. *Chem. Commun.* **2015,** *51*, 7382-7385.

For Table of Contents Use Only

Reduced Grapheme Oxide Membrane induced Robust Structural Colors towards Personal Thermal Management

Zhijie Zhu,[†‡] *Jing Zhang,*[†‡] *Yu-long Tong,*[†‡] *Gang Peng,*[†‡] *Tingting Cui,*[†‡] *Cai-Feng Wang,*[†‡] *Su Chen**[†‡] *and David A. Weitz**[§]

Table of Contents Graphic

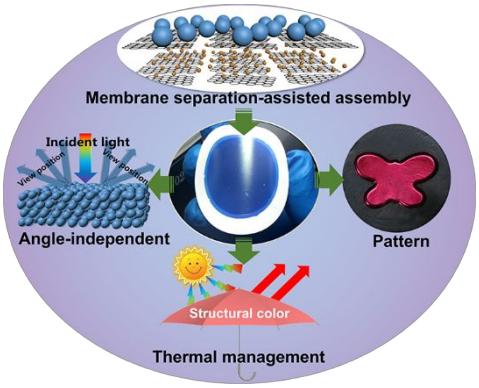

We introduce a membrane separation-assisted assembly of colloidal particles into structural colors. These structural colors are angle-independent because of the amorphous arrangement of particle arrays. Also, an application of thermal management is demonstrated by taking advantage of the inherent slow photon effect.